Journal of Theoretical and Applied Information Technology
10th January 2013. Vol. 47 No.1

ISSN: 1992-8645 www.jatit.org E-ISSN: 1817-3195

STATIC ANALYSIS OF WAVELENGTH TUNING IN TWO SECTION INDEX COUPLED DFB LASERS USING THE TRANSFER MATRIX METHOD

[1]H.BOUSSETA, [2]A.ZATNI, [3]A.AMGHAR, [4]A.MOUMEN, [5]A.ELYAMANI

[1,4,5]PhD Student, M.S.I.T Laboratory, Department of Computer Engineering, high school of technology, Ibn Zohr University, Agadir Morocco.

[2]Prof., Department of Computer Engineering, high school of technology, Agadir Morocco

[3]Prof., Department of physics, faculty of sciences, Ibn Zohr university, Agadir Morocco

E-mail: [1] hamza.bousseta@gmail.com

ABSTRACT

The wavelength tuning is an important issue for distributed feedback (DFB) lasers designs and applications. In this paper we have presented an algorithm to analyze the wavelength tuning characteristics of two-section index-coupled (TS-IC) DFB lasers in above threshold regime, by the means of the transfer matrix method (TMM), and the carrier rate equation. The versatility of the theoretical model in the present work is demonstrated in an analysis of static characteristics of TS-IC-DFB lasers, which illustrated the important influence of coupling coefficient, cavity condition and injection current on the wavelength tuning. Therefore, The TS-IC-DFB lasers will be useful in optical communication systems using wavelength division multiplexed (WDM) networks.

Keywords: *Wavelength Tuning, Distributed Feedback (DFB) Lasers, Transfers Matrix Method (TMM), Static Characteristics.*

1. INTRODUCTION

Wavelength-division-multiplexing (WDM) network need key component with high quality such as highly stable and high output power laser light source [1-2]. The distributed feedback DFB semiconductor laser is one of the fine light sources and has been widely used in optical fiber communication systems, and this is because of their small size, low power consumption, high-speed modulation capability, ultra low threshold current and possible integration with other optical functional devices [3-6].

In Optical communication systems, the static characteristics of DFB semiconductor laser such photon density, carrier density and refractive index [5-7] are important parameters that should be properly predicted. Thereby, to simulated the static effects in the semiconductor DFB lasers, It is common to use a transfer-matrix-method (TMM) [8-9] based on the counter propagation coupled mode equations [8-10], in addition to the carrier rate equation [11].TMM was first proposed by BJORK and NILSSON [12] and the first team using it for analyzing the transmission and reflection gains in the laser amplifiers with corrugated structures was YAMADA and SUMATSN [11].

The tunable semiconductor lasers like DBR lasers [8] [13] [14] [15], DFB laser and other types of lasers had relatively simple tuning Mechanisms, and have been fully theoretically analyzed [8] [16], thus some papers also discussed the wavelength tuning proprieties of multi-electrodes DFB [17]. However the DFB laser cannot achieve as good tuning as DBR lasers, but DFB types do not give a large line-width or rather FM noise and probably also did not gave high speed[18-22].

In this paper, the wavelength tuning properties of the two section index-coupled TS-IC-DFB lasers are discussed and numerically demonstrated. The approach that we presented for the analysis of our device is comprehensive and can well be used to treat other tunable semiconductor lasers. The object of our work is to present TMM capable of simulating the wavelength tuning characteristics in TS-IC-DFB lasers, so this paper is organized as follows: section 2 is devoted to describe in detail

ISSN: 1992-8645 www.jatit.org E-ISSN: 1817-3195

the model and theory of analysis in the frame of TMM. Section 3: we study the wavelength tuning characteristics, taking into account the impact of technical and geometric parameters of the TS-IC-DFB laser such as coupling coefficient, facet reflectivity, current injection and the cavity length. Section 4: comprises the conclusion of this paper.

2. TRANSFER MATRIX METHOD FOR TWO-SECTION INDEX COUPLED DFB LASERS

The two section index-coupled DFB laser investigated in this work is depicted schematically in fig.1. It is consists of two sections, section A and section B, with independent injection. The first section (section A) extends from z=0 to z=L/2, the second section (section B) from z=L/2 to z=L.

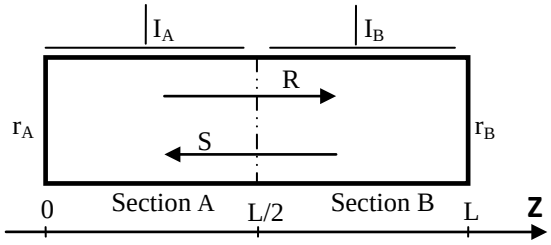

Fig.1. Schematic Diagram Of A TS-IC-DFB Laser

The basis of the transfer matrix method is to divide the laser longitudinally into a number of sections, and in each section the structural and material parameters are assumed to be homogenous.

Each section is then described by a 2 by 2 complex transfer matrix, which represents the relation between forward and backward propagation waves. The transfer matrix of the corrugated section between z_{i+1} and z_i can be pressed by [11].

$$T(z_{i+1}/z_i)=\begin{bmatrix} t_{11}(z) & t_{12}(z) \\ t_{21}(z) & t_{22}(z) \end{bmatrix} \quad (1)$$

Where $z_i = i\frac{L}{M} = i\Delta z$. L is the length of the cavity and M is the total number of sub-sections.

In each sub-section all parameters are assumed constant. So, the forward and the backward propagating waves in each sub-section are related to the next sub-section by the matrix

$$\begin{bmatrix} R(z_{i+1}) \\ S(z_{i+1}) \end{bmatrix} = T(z_{i+1}/z_i)\begin{bmatrix} R(z_i) \\ S(z_i) \end{bmatrix} \quad (2)$$

$R(z)$ and $S(z)$ are the slowly-varying amplitudes of forward and backward propagating fields, and the elements of transfer matrix are given by :

$$t_{11}(z_i)=\frac{\left(E^{+}-\rho^2 E^{-}\right)}{1-\rho^2}e^{-j\beta_o z}e^{j\Omega} \quad (3)$$

$$t_{12}(z_i)=\frac{-\rho\left(E^{+}-E^{-}\right)}{1-\rho^2}e^{-j\beta_o z}e^{-j\Omega} \quad (4)$$

$$t_{21}(z_i)=\frac{\rho\left(E^{+}-E^{-}\right)}{1-\rho^2}e^{j\beta_o z}e^{j\Omega} \quad (5)$$

$$t_{22}(z_i)=\frac{-\left(\rho^2 E^{+}-E^{-}\right)}{1-\rho^2}e^{j\beta_o z}e^{-j\Omega} \quad (6)$$

Where β_0 is the propagation constant, given by:

$$\beta_0 = \pi/\Lambda \quad (7)$$

And $$E^{\pm}(z_i)=e^{\pm\gamma(z_{i+1}-z_i)} \quad (8)$$

Λ is the grating period of the DFB laser, Ω is the phase discontinuity between section i+1 and i, and ρ is given as:

$$\rho(z_i)=\frac{jk}{\alpha(z_i)-j\delta(z_i)+\gamma(z_i)} \quad (9)$$

Where γ is the complex propagation, given by:

$$\gamma(z_i)=\sqrt{\left(\alpha(z_i)-j\delta(z_i)\right)^2+k^2} \quad (10)$$

With α and δ are respectively, the gain and detuning for the propagation modes taking the left section as a reference, k is the complex coupling constant.

For TS-IC-DFB laser had a uniform cavity, one must determine both the amplitude gain coefficient α, and the detuning coefficient δ for the section i in order that each matrix elements $t_{jm}=(j,m=1,2)$ as shown in equations (3)-(4)-(5) and (6) can be determined. For a grating with a

ISSN: 1992-8645 www.jatit.org E-ISSN: 1817-3195

first-order bragg diffraction, the mode detuning and the gain can be expressed respectively for an arbitrary section i by [11]:

$$\delta(z_i) = \frac{2\pi}{\lambda} n(z_i) - \frac{2\pi n_g}{\lambda\lambda_B}(\lambda - \lambda_B) - \frac{\pi}{\Lambda} \quad (11)$$

And

$$\alpha(z_i) = \frac{\Gamma g(z_i) - \alpha_s}{2} \quad (12)$$

Where λ is the lasing mode wavelength, λ_B is the bragg wavelength, n_g is the group refractive index, n is the refractive index, α_s is the constant cavity loss, Γ is the optical confinement factor, and the material gain g for semiconductors is expressed as[7]:

$$g(z_i) = A_0(N(z_i) - N_0) - A_1[\lambda - (\lambda_0 - A_2(N(z_i) - N_0))]^2 \quad (13)$$

With A_0 is the differential gain, N is the carrier concentration, N_0 is the carrier density at transparency, λ_0 is the peak wavelength at transparency, A_1 and A_2 and are parameters used in the parabolic model assumed for the material gain.

The effective refractive index can be expressed as [7]:

$$n(z_i) = n_o + \Gamma \frac{dn}{dN} N(z_i) \quad (14)$$

Where n_0 is the refractive index and $\frac{dn}{dN}$ is the differential index.

On the other hand, the average carrier density in the active region along the laser cavity is described by the carrier rate equation as [11]

$$\frac{I_{A,B}}{qV} = R(z_i) + R_{st}(z_i) \quad (15)$$

With

$$R(z_i) = \frac{N(z_i)}{\tau} + BN^2(z_i) + CN^3(z_i) \quad (16)$$

$$R_{st}(z_i) = \frac{C_g g(z_i) P(z_i)}{1 + \varepsilon P(z_i)} \quad (17)$$

Where $I_{A,B}$ is the uniform current bias of section denoted by the subscript. q is the electron charge, V is the cavity volume, the parameter τ stands for the electron lifetime, B and C are bimolecular and auger recombination coefficient respectively, $C_g = c/n_g$ is the group velocity, with c is the speed of light in vacuum, and ε is a non-linear coefficient to take into account saturation effects.

The photon density $p(z_i)$ is given by [11]

$$P(z_i) = \frac{2\varepsilon_o n(z_i) n_g \lambda}{hc} c_0^2 \left[|R(z_i)|^2 + |S(z_i)|^2 \right] \quad (18)$$

Where ε_o is the free space permittivity, h is the Planck's constant and c_0 a dimensionless coefficient that allows the determination of the total electric field at the above-threshold regime, taking into account that the normalization

$$|R(0)|^2 + |S(0)|^2 = 1 \quad (19)$$

From the threshold studies [7] [11], the threshold carrier concentration N_{th} can be obtained from equations (11) – (12), and such that

$$N_{th} = N_0 + (\alpha_s + 2\alpha_{th}) / \Gamma A_0 \quad (20)$$

At threshold conditions, we assumed that the $A_1 = A_2 = 0$ and $\delta = \delta_{th}$, consequently from equation (10), we can express the threshed refractive index and the threshold wavelength such that [11]:

$$n_{th} = n_0 + \Gamma \frac{\partial n}{\partial N} N_{th} \quad (21)$$

$$\lambda_{th} = \frac{2\pi\lambda_B (n_g + n_{th})}{\delta_{th}\lambda_B + 2\pi n_g + \lambda_B \pi / \Lambda} \quad (22)$$

The boundary conditions are described by:

$$R(0) = r_A e^{-j\beta_B L} S(0) \quad (23)$$

$$R(L) = r_B e^{-j\beta_B L} S(L) \quad (24)$$

Where r_A and r_B are the facet reflectivity of sections A and B, respectively. β_B is the bragg condition.

ISSN: 1992-8645 www.jatit.org E-ISSN: 1817-3195

3. SIMULATIONS RESULTS AND DISCUSSIONS

In this paper, the numerical procedure for the above-threshold calculations follows closely the algorithm developed in [11], it is used only for a DFB laser with a single electrode, but in our work we have been developing it for the case of a DFB laser with two electrodes. The algorithm was implemented using the programming language C++. A flowchart of the numerical algorithm can be explained by Fig.2, which illustrates how all the various mechanisms are related to one another, each step of this flowchart is a sub program elementary with its own algorithm.

Table 1: Parameters Values Used In Simulations.

Symbol	Parameter	Value
B	Bimolecular recombination	1.10^{-16} m^3 s^{-1}
C	Auger recombination	16.10^{-41} m^6 s^{-1}
τ	Carrier lifetime	4.10^{-9} s
A_0	Differential gain	$2.7.10^{-20}$ m^2
A_1	Gain curvature	$1.5.10^{19}$ m^3
A_2	Differential peak wavelength	$2.7.10^{-32}$ m^3
α_s	Internal loss	3.10^3m^{-1}
r_0	Refractive index at zero injection	3.413515
N_0	Carrier concentration at transparency	$1.2.10^{24}$ m^{-3}
dn/dN	Differential index	$-1.8.10^{-26}$ m^3
C_g	Croup velocity	8.11 10^7 m.s^{-1}
ε_0	Non linear gain coefficient	$1.5.10^{-23}$ m^3
W	Active layer width	2.10^3 nm
D	Active layer thickness	$0.15.10^3$ nm
Γ	Optical confinement factor	0.35
Λ	Grating period	227.039 nm
λ_B	Bragg wavelength	1550 nm
λ_0	Peak gain wavelength at transparency	1569.1 nm
I_{th}	Threshold current	21.84 mA

With the modeling described in second section, the static tuning characteristics of TS-IC-DFB laser were simulated and demonstrated with the parameters given in table1.

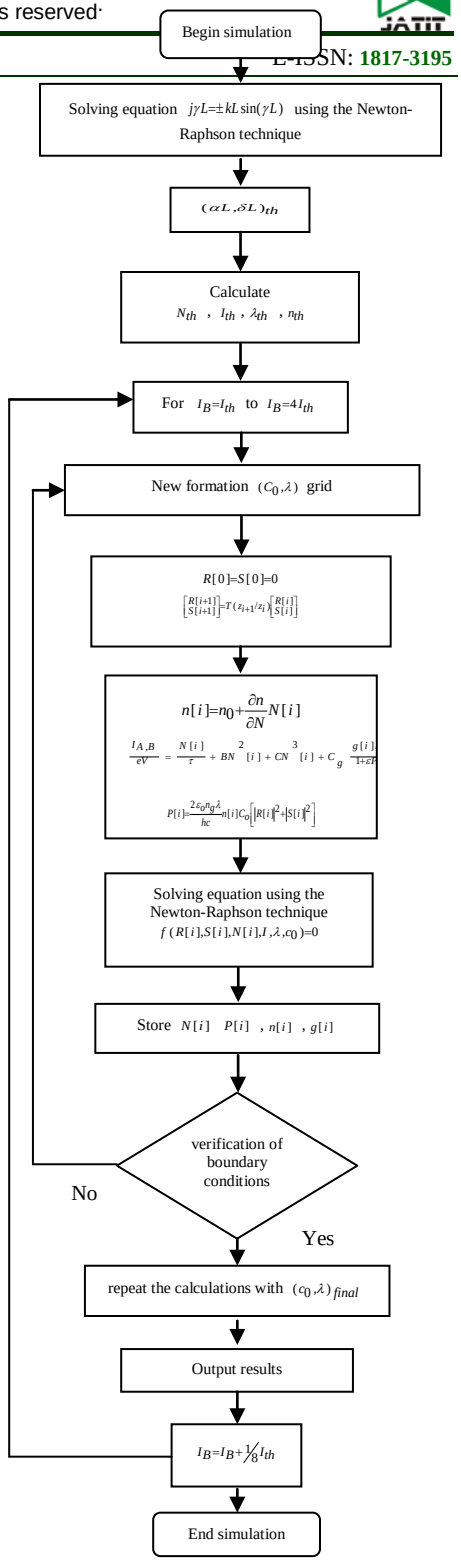

Fig.2. Flowchart Of Static Numerical Algorithm.

We evaluated the longitudinal distribution of the carriers and photons along the cavity by dividing the cavity length into sub-sections of equal length. In our simulations a large number of transfer matrices must be used for a 300µm long DFB laser, at least 300 transfer matrices have been adapted to

Journal of Theoretical and Applied Information Technology
10th January 2013. Vol. 47 No.1

ISSN: 1992-8645 www.jatit.org E-ISSN: 1817-3195

evaluate the static characteristics of our device. For demonstration of the tuning mechanism, when the currents are pumping asymmetry, it is interesting to see under different bias conditions the evolution of photon density, carrier density and refractive index in the cavity. All results are shown in Fig.3.

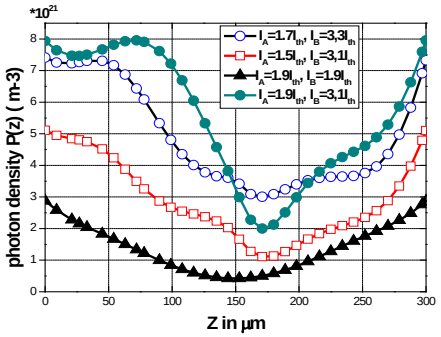

(a)

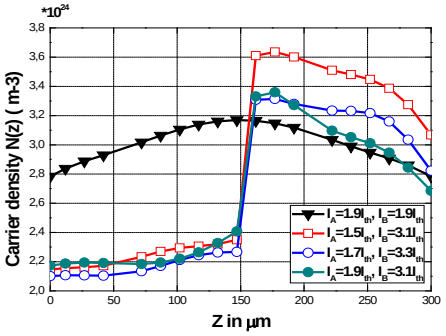

(b)

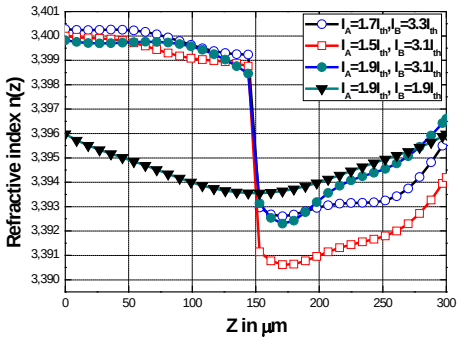

(c)

Fig.3. Longitudinal Distribution Of (A) Photon Density, (B) Carrier Density, (C) Refractive Index In TS-IC-DFB Lasers For Different Biasing Currents, With L=300µm And Kl=2.

The photon localization is controllable by changing the current injection ratio between different sections, this may cause a wavelength shift. Thereby, when the current increase, the longitudinal of the photon density and carrier density also increase for all pairs of current, Fig .3.a and b, respectively shows photon density and the carrier concentration profiles. On the other hand the variations of the spatially distributed refractive index are illustrated in Fig.3.c. We observe that the refractive index decreases when the current also increases, i.e. when the photon density increases. All measurement of Fig.3, were conducted with a geometry of L=300µm and kL=2. In order to provide a deeper understanding the wavelength tuning characteristics, we present the effects of coupling coefficient, cavity condition and injections currents on the wavelength tuning.

The wavelength tuning characteristics are shown in fig.4, with $I_A=1.7I_{th}$ (a), $I_A=1.9I_{th}$ (b), $I_A=2.5I_{th}$ (c). Therefore, we have the emission wavelength λ(µm) as a function of the injection current in section B, where kL=2 and L= 500 µm

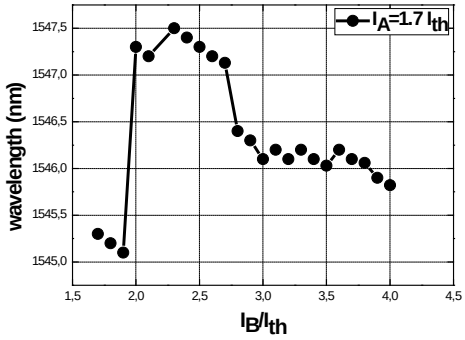

(a)

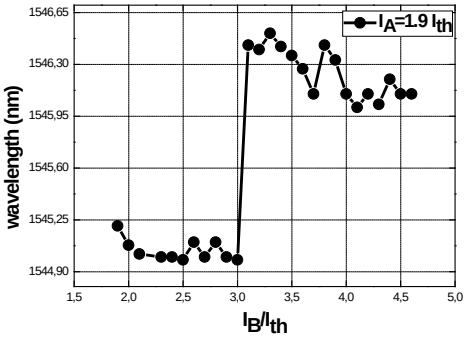

(b)

Journal of Theoretical and Applied Information Technology
10th January 2013. Vol. 47 No.1

ISSN: 1992-8645 www.jatit.org E-ISSN: 1817-3195

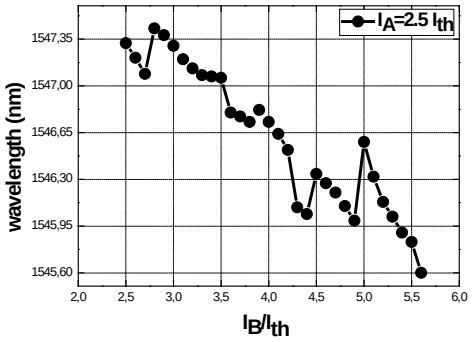

(c)

Fig.4. Wavelength Tuning Characteristics Of TS-IC-DFB Lasers For Different Biasing Currents Of Section A, (A) $I_A=1.7I_{th}$, (B) $I_A=1.9I_{th}$, (C) $I_A=2.5I_{th}$, With L=500 Mm And Kl=2.

When the injection current in the section A as $I_A=1.7I_{th}$, we observe that the emission wavelength varies discontinuously. We get 8 continuous tuning ranges with a maximum tuning range of 0.41nm. These ranges are separated by mode hopping. However, when the injection current in the first section as $I_B=1.9I_{th}$ or $I_B=2.5I_{th}$ .in this case, a clear reduction of the tuning range is obtained ,we get only 7 continuous tuning ranges, with a maximum tuning range of 1nm. This is caused by the low injected carrier density in the cavity. We can say that the wavelength is electronically tuned by the currents.

The Fig.5 Shows the wavelength tuning characteristics for different lengths of the cavity depending on the current I_B, with $I_A=1.8I_{th}$ and kL=2. The maximum tuning range 1.1nm, 0.7nm and 0.4nm are obtained for the cavities of lengths as L=300µm, L=400µm and L=500µm ($L_A=L_B=L/2$) respectively. For the same bias current, its density increases when we reduce the length of the cavity, which increases the carrier density inside the cavity. This explains that for the same excursion of current, a large range of tenability is obtained with the shortest lasers.

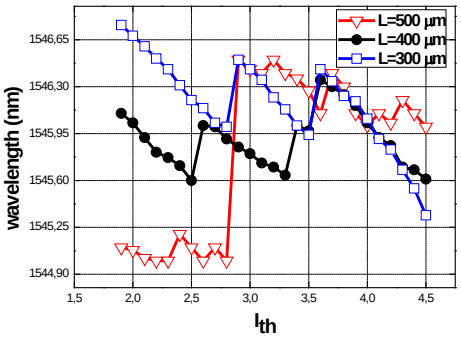

Fig.5. Wavelength Tuning Characteristics Of TS-IC-DFB Lasers For Different Lengths Of The Cavity, With $I_A=1.8I_{th}$ And Kl=2.

The Fig.6 shows the evolution of the emission wavelength λ(µm) as a function of the injection current in section B, When the injection current in section A is fixed at $l_A= 2l_{th}$. So, the figure compares the wavelength tuning characteristics of two lasers for two different coupling coefficients (kL=2 and kL=4) and for the same injection currant. If the coupling coefficient is kL=2, we observe that the number of the continuous tuning is decreases and the overall tuning range is extended to 0.73nm.

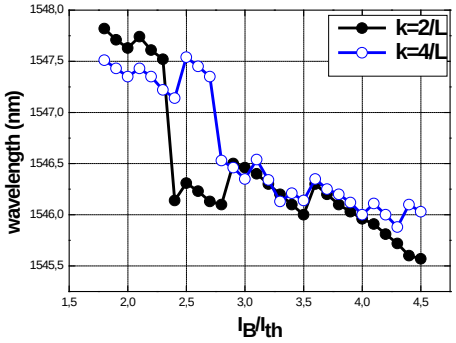

Fig.6. Wavelength Tuning Characteristics Of TS-IC-DFB Lasers For Different Values Of Coupling Coefficients, With $I_A=2I_{th}$ And L=500 Mm.

Finally, to show The dependence of the wavelength tuning on facet reflectivity the device is simulated for different values of first facet reflectivity r_A, with facet reflectivity $r_B=0$, thus the results are shown in Fig.7.

ISSN: 1992-8645 www.jatit.org E-ISSN: 1817-3195

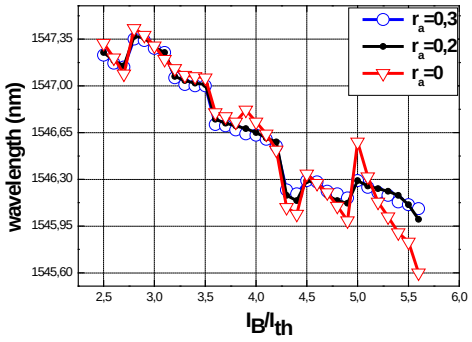

Fig.7. Wavelength Tuning Characteristics Of TS-IC-DFB Lasers For Different Values Of Facet Reflectivity Of Section A, With I_A=2.5Ith, L=500 And Kl=2.

4. CONCLUSION

With a more efficient algorithm based on TMM and carrier rate equation, we have investigated the wavelength tuning characteristics of TS-IC-DFB laser. Furthermore, the longitudinal distribution of photon density, carrier density, reflective index as well as losing wavelength was presented. We have also analyzed the effects caused by changing structural parameters on wavelength tuning, a maximum tuning range of 1.1 nm in our laser has been observed .We believe that more devices can also be analyzed using TMM and will form the subject of a future study.

REFRENCES:

[1] A. Zatni, D. Khatib, M. Bour J. Le bihan, " Analysis of the spectral stability of the three pahse shift DFB laser (3PS-DFB)", *Annals of telecommunication*, vol. 59, 2004, pp.1031-1044.

[2] M. saeed Tahvili, M. Hossein Sheikhi, "steady state analysis of optical bistability in distributed coupling coefficient DFB semiconductor laser amplifiers", *Solid-state Electronics*, vol.53, 2009, pp. 79-85.

[3] M.Jabbari, M.K. Moravvej Farshi, R. Ghayour, A. Zarifkar, "SPM response of a distributed coupling coefficient DFB-SOA all- optical flip-flop", *Majlesi Journal of Electrical Engineering*, vol.4,No=.1, 2010, pp. 1-6.

[4] Olaf Brox, Stefan Bauer, Mindaugas Radziunas, Matthias Wolfrum Wolfrum, Tan Sieber, Jochen Kreissl, Bernd Sartorius and hans-jurgen Wunsche, "High-frequency pulsation in DFB lasers with amplified feedback", *IEEE journal of Quantum Electronics*, vol.39,No.11, 2003, pp. 1381-1387.

[5] A. Moumen, A. Zatni, A. elkaaouachi, H. Bousseta, A. Elyamani, "A novel design of quarter wave-shifted diqstributed feedback semiconductor laser for high-power single - mode operation", *JATIT Journal of theoretical and applied information technology*, Vol. 38, No. 2, 2012, pp. 210-218.

[6] M.G. Davis, R.F. O'dowd, " A transfer matrix method based large-signal dynamic model for multielectrode DFB lasers", *IEEE journal of Quantum Electronics*, vol.30, 1994, pp. 2458-2466.

[7] josé A.P. Morgado, Carlos A.F. Fernandes, josé B.M. Boavida, " novel DFB structure suitable for stable single longitudinal mode operation", *Optics & Laser technology*, vol.42, 2010, pp. 975-984.

[8] Kai Shi, Yonglin Yu, Ruikang Zhang, Wen Liu, Liam P. Baryy,"Static and dynamic analysis of side-mode suppression of widely tunable sampled grating DBR (SG-DBR) lasers", *optics communications*, vol.282, 2009, pp. 81-87.

[9] Drew N. Maywar, Govind P. Agrawal, "Transfer-matrix analysis of optical bistability in DFB semiconductor laser amplifiers with nonuniform gratings", *IEEE journal of Quantum Electronics*, vol.33, 1997.pp. 2029-2037.

[10] M.G. Davis, R.F. O'dowd, "A transfer matrix method based large-signal dynamic model for multielectrode DFB lasers", *IEEE journal of Quantum Electronics*, vol.30, 1994, pp. 2458-2466.

[11] H. ghafouri-shiraz, distributed feedback laser diodes and optical tunable filters, Birmingham, UK : WILEY ,2003

[12] Gunnar Bjork, Olle Nilsson, *IEEE J. Lightwave Techno*. LT-5.1987, pp. 140-148.

[13] A. Zatni, J. Le bihan, "Analysis of FM and AM responses of a tunable three-electrode DBR laser diode", *IEEE journal of Quantum Electronics*, vol.31 ,1995, pp.1009-1014.

[14] Giora Griffel, Robert J.Lang, Amnon Yariv, " Two-Section Gain-Levered tunable distributed feedback laser with active tuning section", *IEEE journal of Quantum Electronics*, vol.30, 1994, pp. 15-18

ISSN: 1992-8645 www.jatit.org E-ISSN: 1817-3195

[15] J.B. Ekanayake and N. Jenkins, "A Three-Level Advanced Static VAR Compensator", *IEEE Transactions on Power Systems*, Vol. 11, No. 1, January 1996, pp. 540-545.

[16] Tien-Pei Lee, "recent advances in long-wavelength semiconductor lasers for optical fiber communication", *proceeding of the IEEE*, vol. 79.No.3, 1991, pp. 253-276.

[17] Nong Chen, Yoshiaki Nakano, Kazuya Okamoto, Kunio Tada, Geert I. Morthier, Roel G. Baets, "Analysis, fabrication, and characterization of tunable DFB lasers with chirped gratings", *IEEE journal of Quantum Electronics*, vol.3, NO.2, 1997, pp541-546.

[18] Mahmoud Aleshams, M.K. Moravvej-Farshi, M.H.Sheikhi, "Tapered grating effects on static properties of a bistable QWS-DFB semiconductor laser amplifier", *Solid-state Electronics*, vol.52, 2008, pp.156-163.

[19] Xin-Hong Jia, Dong-Zhou Zhong, Fei Wang, Hai-Tao Chen, "Detailed modulation response analyses on enhanced signal-mode QWS-DFB lasers with distributed coupling coefficient", ", *optics communications*, vol.277, , 2007, pp. 166-173.

[20] S. K. B. Lo, H. Ghafouri-shiraz , "A method to determine the above-threshold stability of distributed feedback semiconductor laser diodes",
journal of lightwave technology, vol.13, 1995, pp. 563-576.

[21] F.Shahshahani and V.Ahmadi, "analysis of relative intensity noise in tapered grating QWS-DFB lasers diodes by using three equations model", *Solid-state Electronics*, vol.52, 2008. pp. 857-862,

[22] A. Zatni, "Study of the short pulse generation of the three quarter wave shift DFB laser (3QWS-DFB)", *Annals of telecommunication*, vol.60, 2005. pp. 698-718.